axial electric field. In this region the $j_\theta B_r$ force serves to hold the mass layer together but little mass acceleration is possible.

The current is carried by electrons only. The E_θ force on the ions is balanced by the resistivity force of the current carrying electrons so that no θ velocity develops. The E_z force is adequate to account for the axial motion with no requirement for an additional $V_\theta B_r$ force. The electron density distribution calculated by numerical integration of the general Ohm's Law relation, containing the electron density gradient, is consistent with the laser measured distribution and provides a consistent interpretation of all of the probe data.

References

[1] Lovberg, R. H., "Acceleration of Plasma by Displacement Currents Resulting from Ionization," *Proceedings of the VI International Conference on Ionization Phenomena in Gases*, Vol. IV, Faculté des Science de Paris, 1963, pp. 235–239.

[2] Dailey, C. L., "Plasma Properties in an Inductive Pulsed Plasma Accelerator," AIAA Paper 65-637, Evanston, Ill., 1965.

[3] Bodin, H. A. B., et al., "The Influence of Trapped Field on the Characteristics of a Magnetically Compressed Plasma (Thetatron)," *Nuclear Fusion*, 1962 Supplement, Pt. 2, pp. 521–532.

[4] Bodin, H. A. B. and Newton, A. A., "Rotational Instability in the Theta Pinch," *The Physics of Fluids*, Vol. 6, No. 9, Sept. 1963, pp. 1338–1345.

[5] Dailey, C. L., "Plasma Rotation in a Pulsed Inductive Accelerator," *Proceedings of the XVII Astronautical Congress*, PWN-Polish Scientific Publishers, Vol. III, 1966, pp. 253–260.

[6] Lovberg, R. H., "Investigation of Current Sheet Microstructure," AIAA Paper 65-335, San Francisco, Calif., 1965.

[7] Dailey, C. L., "Investigation of Plasma Rotation in a Pulsed Inductive Accelerator," *AIAA Journal*, Vol. 7, No. 1, Jan. 1969, pp. 13–19.

[8] Spitzer, L., *Physics of Fully Ionized Gases*, Interscience, New York, 1956.

[9] Siemon, R. E., "Current Sheet Structure in a Low Energy Theta Pinch," Ph.D. thesis, 1969, Univ. of California, San Diego.

[10] Salpeter, E. E., "Electron Density Fluctuation in a Plasma," *Physical Review*, Vol. 120, No. 5, 1960, pp. 528–535.

FEBRUARY 1972 AIAA JOURNAL VOL. 10, NO. 2

Roll Resonance and Passive Roll Control of Magnetically Stabilized Satellites

R. W. KAMMÜLLER*
European Space Research and Technology Centre, Noordwijk, Holland

The resonant roll solutions of the magnetically stabilized satellite are investigated using a variational approach. The variational problem is solved by the numerical method of Ritz. A parameter study is made for the case of the satellite ESRO I. The basic properties of the different classes of solution are discussed. Emphasis is laid on the class of rotational solutions. A policy for the optimal selection of the inertial parameters is defined. The optimized spacecraft sustains stable rotational roll motions. The policy allows control of the class of roll motions in a passive way. The results of the analysis generally agree with observed ESRO I flight data.

1. Introduction

THE type of satellite considered here belongs to the class of spacecraft oriented by magnetic means.[1] The control principle as illustrated in Fig. 1, represents a passive one-axis control. A simple permanent magnet, fixed rigidly to the structure of the spacecraft, is used to align the reference axis (Z axis) of the satellite to the local direction of the Earth magnetic field. A number of ferromagnetic rods placed normal to the reference axis are applied to damp the libration motions of the satellite. This type of control is usually chosen to orient small scientific satellites designed for auroral and ionospheric studies in near-polar orbits. Owing to the dipole character of the geomagnetic field, the orbiting spacecraft is forced to perform a "head-over-heels" motion around its lateral axis. This motion shall later be called the pitch motion whereas the motion around the reference axis shall be denoted as the roll motion of the spacecraft. In a previous paper the residual roll motion for the general non-symmetrical rigid body has been analyzed and the appearance of resonant roll solutions has been predicted.[2] It could be shown that the roll resonance effect is parametrically excited by the non-uniform components of the pitch motion, the mechanism for the exchange of energy between pitch and roll motion being provided by inertial crosscoupling. By use of a perturbation method the existence of a large variety of harmonic and subharmonic solutions of the oscillatory type could be proven.

The present paper extends the investigations to the class of

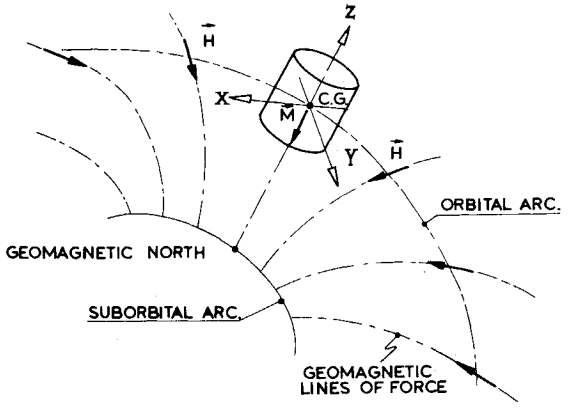

Fig. 1 Orientation of the magnetically stabilized satellite above the northern polar region, M—magnetic dipole moment of satellite, H—local gradient of the geomagnetic field.

Received March 1, 1971; revision received August 12, 1971. Presented at the XXIst International Astronautical Congress, Constance, Germany, October 1970, in abbreviate form.

Index category: Spacecraft Attitude Dynamics and Control.

* Research Engineer, Satellite and Sounding Rockets Department.

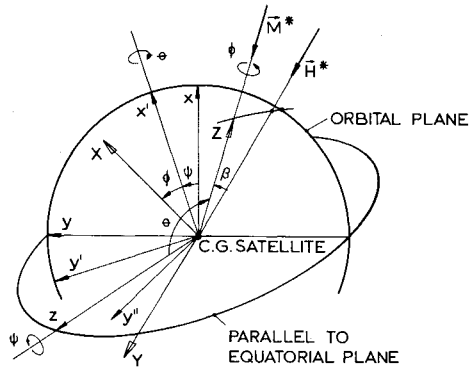

Fig. 2 Definition of Eulerian angles (Ψ, Θ, Φ,) and angular distance β between satellite dipole M* and local field gradient H*.

rotational roll motions. In addition the properties of oscillatory solutions at large amplitudes are analyzed. For the computation of the resonance modes a new method has been applied, which avoids the inherent restrictions of the perturbation technique.[3] Basically the search for the resonant solution is considered as a variational problem which is subsequently solved by the numerical method of Ritz. This technique has shown good convergence and stability properties and is well suited to calculate unstable periodic solutions which are difficult to obtain by direct numerical integration.

In the second part of this paper the manifold of resonant roll solutions and their dependency on the inertia ratio of the satellite are discussed. The question of how far a slow but continuous rotational roll motion can be sustained, is of considerable technical importance due to the influence on the thermal balance of the spacecraft. An attempt therefore was made to define an optimal policy for the selection of the inertial parameters which would permit sustaining of stable rotational roll motions. The principle was applied to the scientific satellites ESRO IA and B. In closing some roll data measured and transmitted by the satellite ESRO IA are presented to show the practical performance of the control principle.

2. The Energy Terms of the Dynamic Model

In describing the attitude behavior of the magnetically oriented satellite the following assumptions are made: the spacecraft shall be considered as a rigid body of dimensions which are small compared to the primary body. Thus the attitude motion is assumed as decoupled from the orbital motion and might be fully described by a dynamic model of three degrees of rotational freedom. The spacecraft is moving on a circular and polar orbit. The magnetic potential of the Earth shall be approximated by a dipole potential as derived in the Appendix. Perturbations due to aerodynamic and gravity-gradient forces are neglected. The frequency range of interest is the range of the orbital frequency and its harmonics. This final assumption shall be explained in more detail below.

Generally there are three ranges of frequencies which are of importance for the attitude behavior of the magnetically oriented satellite: 1) natural frequencies of the transverse axes, $\omega_n \simeq 10^{-2}$ (rad/sec); 2) orbital frequency, $\Omega \simeq 10^{-3}$ (rad/sec); 3) diurnal frequency, $\omega_e \simeq 7.28\ 10^{-5}$ (rad/sec).

Computer simulation and analysis of flight data have shown that roll resonance might take place in ranges 1 and 2. In range 3 no evidence for roll resonance has been found. Roll resonance in region 1 is an internal resonance effect, which can be initiated if the mean roll rate reaches values close to the natural frequency of one of the lateral axis, (roll lock-in). It is a basic requirement for the design of the attitude control system that 1) the natural frequencies ω_n are sufficiently distant from the orbital frequency Ω and 2) the hysteresis damper is able to avoid any internal roll resonance. These problems have been investigated elsewhere.[4]

The present work deals with resonance effects in frequency range 2 which is called the range of externally excited roll resonance. As found earlier[2] it is the forced pitch motion due to the geomagnetic field which sustains the resonance in range 2. The adjacent frequency regions 1 and 3 are sufficiently distant to permit a resonance analysis in region 2 under the following assumptions: 1) Oscillations with natural frequencies of the transverse axes have been damped out, 2) Parameter variations due to the daily rotation of the Earth can be considered as a slowly varying process.

The attitude of the satellite shall be described by the relative position of a body-fixed principle axis system (X, Y, Z) to an orbit-fixed axis system (x, y, z) expressed by the set of Eulerian angles (Ψ, Θ, Φ) as shown in Fig. 2.† The time history of the Eulerian angles $\Psi(t), \Theta(t), \Phi(t)$ is also referred to as pitch, yaw and roll motion. The Z axis has been selected as reference axis of the satellite, the dipole-moment $\mathbf{M}^*$ of the stabilizing magnet is pointing in $-Z$ direction. In view of the following derivations, the energy terms shall be expressed in terms of generalized coordinates, which are readily obtained in form of the classical Euler-angles. It is convenient to introduce the usual letter q_i for the generalized coordinate and define the identity

$$\begin{bmatrix}\Psi\\ \Theta\\ \Phi\end{bmatrix} \equiv \begin{bmatrix}q_1\\ q_2\\ q_3\end{bmatrix} = \mathbf{q} \tag{1}$$

where $\mathbf{q}$ denotes a 3×1 column matrix, corresponding to the 3 degrees of freedom of the attitude model.

The kinetic energy T of the rigid body is found from

$$T = \tfrac{1}{2}\omega^T \mathbf{I} \omega \tag{2}$$

where $\mathbf{I}$ is the diagonalized inertial matrix, the diagonal elements being the three principle moments of inertia A, B, C of the spacecraft. $\boldsymbol{\omega}$ denotes a column matrix composed of the three angular velocity components resolved in the body-fixed frame. Expressing $\boldsymbol{\omega}$ in terms of the generalized coordinates and velocity by

$$\omega = \mathbf{R}\dot{\mathbf{q}} \quad \text{with} \quad \mathbf{R} = \begin{bmatrix} sq_2\, sq_3 & cq_3 & 0\\ sq_2\, cq_3 & -sq_3 & 0\\ cq_2 & 0 & 1\end{bmatrix}$$

one obtains the kinetic energy of the system as the quadratic expression

$$T = \tfrac{1}{2}\dot{\mathbf{q}}^T \mathbf{K} \dot{\mathbf{q}} \tag{3}$$

where $\mathbf{K}$ is the general inertial matrix

$$\mathbf{K} = \begin{bmatrix} (A-B)s^2q_2\, s^2q_3 + Bs^2q_2 + Cc^2q_2 & (A-B)sq_2\, sq_3\, cq_3 & Ccq_2\\ (A-B)sq_2\, sq_3\, cq_3 & (A-B)c^2q_3 + B & 0\\ Ccq_2 & 0 & C\end{bmatrix} \tag{4}$$

(s and c stand for the trigonometric functions sin and cos; the superscript T denotes transposition of a matrix).

The potential energy of the stabilization magnet of the satellite in the local magnetic field of the Earth has been derived in the Appendix. By truncation of the series expansion for the geomagnetic potential approximate expressions are obtained which model the essential time dependencies and yet are still convenient for analytical investigations. Having resolved the local field intensity into the in-plane component H_p and a component normal to the orbital plane H_z, the potential energy follows from Eq. (A7) as

$$U = MH_p \sin q_2 \sin(q_1 - \Gamma) + MH_z \cos q_2 + C \tag{5}$$

The field intensity and the inclination Γ can be represented as Fourier series with respect to the two frequencies ω_e and Ω. The ratio of these frequencies is $\omega_e/\Omega = 7.28\ 10^{-2}$. For resonance investigations near Ω it is thus justified to consider parameters depending on ω_e as slowly varying quantities.[5] This is expressed by defining a second time scale

$$\tau = \omega_e t$$

† The singularities of this Euler system are located at $\Theta = 0 \pm n\pi$; they are to be excluded from the valid range of Θ; the stationary value for Θ at normal control is close to $\pi/2$.

which yields for the latitude Λ

$$\Lambda(\tau) = \Lambda_e - \Lambda_o + \tau$$

The series for $H_p = |\mathbf{H}_p|$ and Γ in the fast time scale t are written as

$$H_p(t) = H_{p0}\left\{1 + \sum_{n=0}^{\infty} h(\tau)_n \cos 2n[\alpha(t)+\zeta(\tau)]\right\}$$
$$\Gamma(t) = \gamma_0 - \sum_{n=1}^{\infty} \gamma_n \sin 2n[\alpha(t)+\zeta(\tau)] \tag{6}$$

The component H_z, the coefficient h_n and the phase ζ are regarded as slowly varying parameters

$$\begin{aligned} H_z(\tau) &= 0.127 H_{p0} \sin\Lambda(\tau) \\ h_n(\tau) &= h_n + k_{nm} \cos 2m\Lambda(\tau) \\ \zeta(\tau) &= \arctan[0.203 \cos\Lambda(\tau)] \end{aligned} \tag{7}$$

The quantities of Eq. (7) can be computed for arbitrary values of τ; for operations on the fast time t they are treated as constants. The numerical examples presented in Chap. 4 have been calculated for the case $\tau = \Lambda_o - \Lambda_e$, which corresponds to those configurations where the magnetic poles of the Earth pass the orbital plane. The influence of the τ-variations on the roll resonance effect is discussed at the end of Chap. 4.

The perturbation due to the gradient of the gravitational field of the Earth shall be estimated. For the satellite oriented according to Fig. 1 the perturbing torque normal to the reference axis is

$$|T_g| \leqslant |\tfrac{3}{2}(\mu/R_s^3)(C-B)\sin 2v|$$

where $\mu = 3.98\ 10^{14}\ \mathrm{m^3 sec^{-2}}$, R_s—orbital radius, v—angle between reference axis and local vertical. The control torque produced by the stabilizing magnet is

$$|T_m| = |(\mathbf{M}^* \times \mathbf{H}^*)| = |M^* H^* \sin\beta|$$

with the notation of Fig. 2.

The maximum value of T_g is reached for $v = 45°$. With the parameters given in Chap. 4, (orbital radius 6880 km, and $(B-C) = 3.2\ \mathrm{kg^2}$) one obtains $T_g = 58.8$ dyn cm. Having a magnet of $M = 2.7\ 10^4\ \mathrm{Gcm^3}$ the control error β_g due to the perturbing torque $T_{g\,\max}$ at the mean orbital field intensity of $H_{\mathrm{mean}} = 0.382\ 0e$ follows as

$$\beta_g \leqslant |T_{g\max}|/|MH_{\mathrm{mean}}| \leqslant 5.7\ 10^{-3}\ \mathrm{rad}$$

The influence of the gravity gradient can therefore be considered as perturbation of secondary order and shall further on be neglected.

Of essential influence on the attitude behavior is the magnetic damper system of the spacecraft. The damping torques are assumed as proportional to the angular velocities. The energy dissipation shall in the following be described by a special "work function" $\bar{W}$:

$$\bar{W} = -\dot{\mathbf{q}}^T \mathbf{D} \mathbf{q} \tag{8}$$

where $\mathbf{D}$ denotes the matrix of the linear damping coefficients. The dash over $\bar{W}$ shall indicate that this "work-function" does not have the properties of a potential, additional conditions have to be satisfied when variational principles are being applied.[6]

3. Computation of the Resonant Solutions

For the computation of the resonant solutions a variational technique has been developed.[3] Using the energy expressions derived in Eqs. (3, 5, and 8) a variational problem can be formulated which is solved by the particular resonance mode sought. The appropriate functional is provided by the extended principle of Hamilton

$$\delta J = \delta \int_0^{T_0} (L + \bar{W})\, dt = 0 \tag{9}$$

where $L = T - U$ denotes the Lagrangian of the system and $\bar{W}$ the work function of the dissipation forces. In order to include W into the functional of Eq. (9), the following conditions have to be imposed: during the process of variation the velocity matrix $\dot{\mathbf{q}}$ of $\bar{W}$ has to be regarded as a purely time-dependent quantity replaced by the matrix function $\mathbf{\Lambda}(t)$, thus yielding for $\bar{W}$

$$\bar{W} = -\mathbf{\Lambda}^T \mathbf{D} \mathbf{q} \tag{10}$$

However the function $\mathbf{\Lambda}(t)$ has to represent the time history of the optimal value of $\dot{\mathbf{q}}$ resulting in the condition

$$\mathbf{\Lambda}(t) = \dot{\mathbf{q}}_{\mathrm{opt}} \tag{11}$$

The integration of the functional (9) is to be extended over the basic period T_o of the resonant solution sought for. Problem (9) together with Eq. (11) has to be considered as variational problem with fixed endpoints and additional condition. The class of admissible functions is restricted by the boundary conditions of the problem. The periodic boundary conditions in time-space for the resonant state of a rotational system are given as

$$q_i(t) = q_i(t + T_o) \qquad \text{for oscillatory solutions} \tag{12a}$$
$$q_i(t) = q_i(t + T_o) \pm 2\pi s \qquad \text{for rotational solutions} \tag{12b}$$

where s denotes an arbitrary integer number. The frequency range of interest is the range 2 of the orbital frequency Ω. According to our assumptions the resonant solutions $q_i(t)$ are to be periodic with the basic period

$$T_o = 2\pi r/2\Omega$$

where 2Ω is the basic frequency of the external excitation on the fast time scale, Eq. (6). The integer r has been introduced to account for possible subharmonic solutions.

The variational problem stated above shall be solved by the method of Ritz. To do so the periodicity conditions (12) have to be transformed to equivalent homogeneous boundary conditions by applying the transformations

$$q_i(t) = q_i^*(t) + q_i(o) \qquad \text{for oscillatory solution} \tag{13a}$$
$$q_i(t) = q_i^*(t) + q_i(o) + v_i \Omega t \qquad \text{for rotational solutions} \tag{13b}$$

Now $q_i^*(t)$ represent purely oscillatory coordinates which satisfy the homogeneous conditions at $[o,\ T_o]$

$$q_i^*(o) = q_i^*(T_o) = 0 \tag{14}$$

The factor $v_i \Omega$ represents the mean rate of the rotational solution expressed in terms of the orbital frequency Ω and the "roll number" v_i, which denotes the number of roll revolutions per orbit. Admissible values for v_i are determined by the periodicity condition (12b), (see Chap. 4c).

According to Ritz the coordinates q_i^* can be approximated by a finite series of $3 \times M$ suitable functions $f_{im}(t)$

$$q_i^* = \sum_m a_{im} f_{im}(t) \qquad i = 1, 2, 3;\ m = 1 \ldots M \tag{15}$$

Each function f_{im} has to fulfil the boundary conditions (14). To ensure the convergence of the method the $\{f_{im}\}$ have to represent a complete sequence for all $t \varepsilon \{0, T_o\}$.[7] Both conditions are satisfied by the following approximation

$$q_i^* = \sum_k \{a_{i(k-1)} \sin(p/r)2\Omega t + a_{ik}[\cos(p/r)2\Omega t - 1]\} \tag{16}$$

where the indices i, k, p take the values

$$i = 1, 2, 3; \quad p = 1, 2, 3 \ldots M/2; \quad k = 2p$$

The coefficients a_{im} are considered as the new unknown parameters of the problem. To minimize the functional J defined in (9), the a_{im} have to satisfy the minimum conditions

$$\delta J/\delta a_{im} = 0 \tag{17}$$

which results in the following system of $3 \times M$ equations for the determination of the parameters $\{a_{im}\}$

$$\int_0^{T_0} \left(\frac{\delta T}{\delta a_{im}} - \frac{\delta U}{\delta a_{im}} + \frac{\delta \bar{W}}{\delta a_{im}}\right) dt = 0 \qquad \begin{matrix} i = 1,2,3 \\ m = 1 \ldots M \end{matrix} \tag{18}$$

For the partial derivatives of the energy terms given in Eqs. (3, 5, and 8) one obtaines the expressions

$$\delta T/\delta a_{im} = \tfrac{1}{2}(\dot{\mathbf{q}}^T[\delta \mathbf{K}/\delta a_{im}]\,\dot{\mathbf{q}} + 2\,\dot{\mathbf{q}}^T \mathbf{K}[\delta \dot{\mathbf{q}}/\delta a_{im}]) \tag{19a}$$
$$\delta W/\delta a_{im} = -\mathbf{\Lambda}^T \mathbf{D}[\delta \mathbf{q}/\delta a_{im}] \qquad i = 1, 2, 3 \tag{19b}$$
$$\delta U/\delta a_{1m} = M\{H_p \sin q_2 \cos(q_1 - \Gamma)\}\, \delta q_1/\delta a_{1m} \tag{19c}$$
$$\delta U/\delta a_{2m} = M\{H_p \cos q_2 \sin(q_1 - \Gamma) - H_z \sin q_2\}\, \delta q_2/\delta a_{2m} \tag{19d}$$
$$\delta U/\delta a_{3m} = 0 \tag{19e}$$

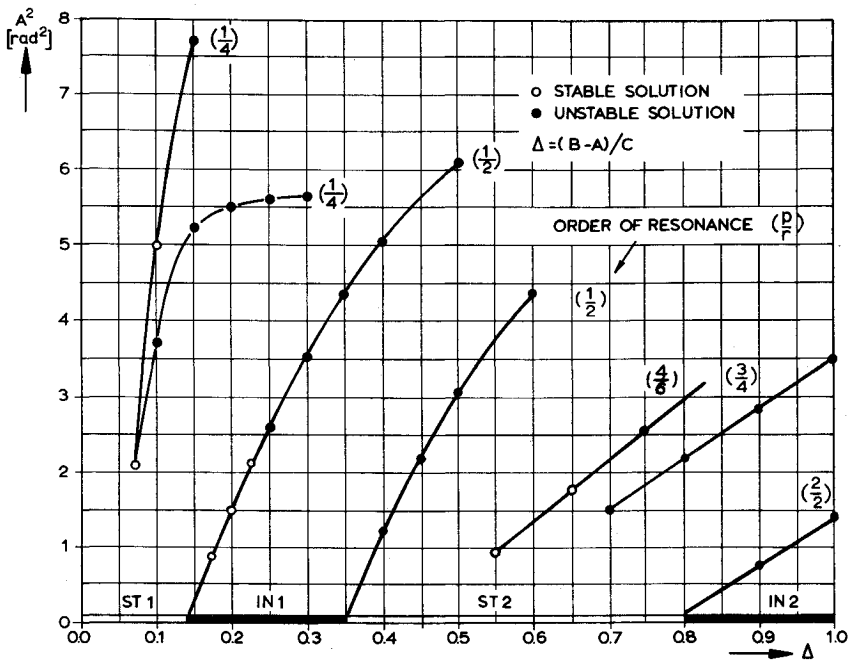

Fig. 3 Amplitude characteristics of the oscillatory roll solution as function of the inertial cross-coupling Δ.

The value for Λ is given by condition (11); all parameters depending on the slow time τ are treated as constants. The coordinates q_i are considered as functions of the set $\{a_{im}\}$ as defined by Eqs. (13) and (16). The square brackets denote matrices having the rank of **K** and **q**, respectibely. The initially unknown boundary values $q_i(o)$ of Eq. (13) can be determined from the three equilibrium conditions for the stationary forces of the system

$$\int_0 \left(\frac{\partial U}{\partial q_i}\right) dt = 0 \qquad i = 1,2,3 \tag{20}$$

The system of Eqs. (18) and (20) has been solved by numerical means using a digital high-speed computer of the type IBM 360/40. The algorithm was based on a least square estimate of the parameter-set $\{a_{im}\}$. If ε_k denotes the error involved in computing the kth equation of system (18) and (20) the minimizing set $\{a_{im}\}$ can be found by solving the problem

$$\text{Min}\,\Sigma_\kappa \varepsilon_\kappa^2[\{a_{im}\}, q_i(o)] \qquad k = 1, \ldots, (3M+3)$$

Good results have been obtained using a regression program developed by Marquardt,[8] the strategy of which resembles an optimal compromise between the Newton method and the gradient method.

4. The Resonant Roll Solution

The roll motion is described by the time history of the third generalized coordinate $q_3(t)$. In previous investigations, Ref. 2, it was found that in presence of damping the satellite finally acquires one of the following basic classes of roll solutions: a) Trivial solution, (nonresonant rest-position); b) Resonant oscillatory solutions; c) Resonant rotational solutions. Inertial coupling was found responsible for the energy exchange between the roll motion and the motion around the lateral axes. The critical parameter for the excitation of resonant roll solutions is the inertial crosscoupling factor Δ of the roll axis, defined as

$$\Delta = (B-A)/C \qquad o < \Delta < 1$$

In the following the basic properties of the three classes of solutions shall be discussed. Special emphasis is laid on the class of rotational solutions. In order to compare the results to those of the aforementioned study, the factor Δ is chosen again as free parameter. The numerical examples have been calculated for the case of the European satellite ESRO 1A, (AURORAE). The fixed parameters of this study take the following values: dipole moment of the stabilizing magnet, $M = 2.7\ 10^4$ g cm^3; second inertia ratio, $B/C = 1.5$; damping coefficient of the roll axis, $d_3/C = 1.10^{-5}\,\text{sec}^{-1}$; orbital frequency, $\Omega = 1.03\ 10^{-3}\,\text{sec}^{-1}$; mean orbital radius, $R_s = 6880$ km. The amplitude characteristics shown in Figs. 3 and 4 have been computed for the slowly varying parameters (7) taken at $\tau = \Lambda_o - \Lambda_e$ (orbit passes over geomagnetic poles). The coefficients h_n, k_{nm} and γ_n are compiled in Table 2 of the Appendix.

a) The trivial solution for the roll angle $q_3 = 0$ corresponds to the nonresonant rest position of the satellite defined by $\Phi_o = 0 \pm n\pi$. The spacecraft is performing a pure pitch motion, the axis of maximum moment of inertia pointing normal to the orbital plane. For those values of the crosscoupling factor Δ which are located inside the regions, ST1, ST2 on the Δ scale of Fig. 3, the rest position is of limited asymptotic stability. Relatively small perturbations $(\delta\phi, \delta\dot{\phi})$ are sufficient to transfer the system to a class b or c of solution. When the factor Δ belongs

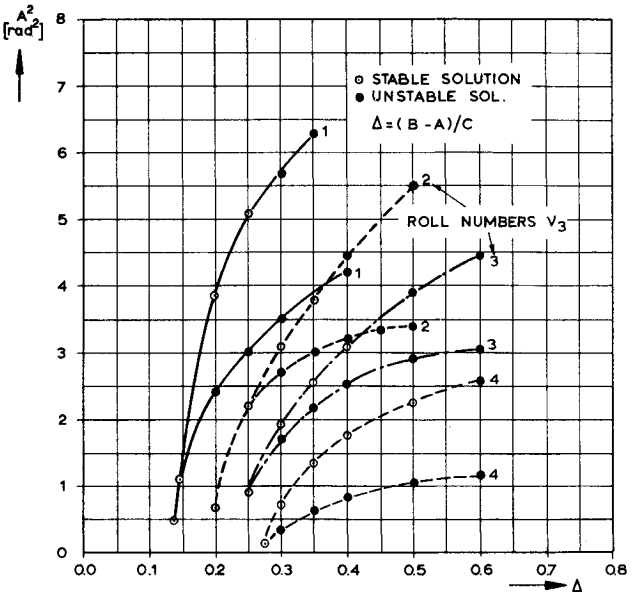

Fig. 4 Amplitude characteristics of the rotational roll solutions. ν_3—roll number in revolution per orbit.

to either region IN1 or IN2 the trivial roll solution is of unstable nature in spite of the energy dissipation in the damper system. These results are in excellent agreement with those obtained by the perturbation method.[2]

b) The resonant oscillatory solution consists of a purely periodic roll oscillation as described in Eq. (13a)

$$q_3 = q_3{}^*(t) + q_3(0)$$

The amplitude characteristics of the most important modes are plotted in Fig. 3. It shows the square amplitude $A^2 = a_{3\kappa}^2 + a_{3\kappa-1}^2$ of the dominating sin- and cos-term of the periodic solution as a function of the factor Δ. Each characteristic is labeled by the order of resonance (p/r) from which follows the basic frequency of the solution as $\omega_o = 2\Omega/r$ and the frequency of the dominating term as $\omega_p = 2\Omega(p/r)$.

For small roll amplitudes ($A < 1$) the results agree, as expected, with those found by the perturbation method.[2] For large amplitudes a number of new features have been found. Firstly the dependency of A on Δ does no longer follow a square law but results in a considerable flattening of the characteristics for $\Delta \to 1$. The splitting of each amplitude curve of a particular order (p/r) into two branches has been verified. But the upper branch does comprise only a closed region of stable solutions. There exists an upper limit beyond which no stable amplitudes are found. The lower branch of the amplitude curve represents unstable solutions on its whole length. For example, the full set of amplitudes $\{a_{3m}\}$ for a typical 14-term oscillatory solution is presented in Table 1, case $v_3 = 0$.

c) The rotational solution represents a speciality of rotating systems. The general form is given with Eq. (13b) as

$$q_3 = q_3{}^*(t) + q_3(0) + v_3\Omega t$$

where the "roll number" v_3 defines the roll revolutions per orbit. First the necessary conditions for external excitation of rotational roll modes shall be summarized. It was found by numerical experiment that the series $H(t)$ and $\Gamma(t)$ of Eq. (6) which are the external forcing terms of the system, have to compromise certain harmonic terms. In order to sustain rotational solutions with a mean roll rate $v_3\Omega$ at least one of the terms

$$\gamma_{2v3}\cos 2v_3\Omega t \quad \text{or} \quad h_{2v3}\cos 2v_3\Omega t$$

has to appear in the series of Eq. (6); in other words the condition

$$\gamma_{2n} \neq 0 \quad \text{and/or} \quad h_{2n} \neq 0 \quad \text{for} \quad v_3 = n \qquad (21)$$

has to hold.

A second condition can be derived from the necessary interrelation between mean roll rate and superimposed oscillation.

Table 1 Five examples for the amplitude set (a_{3m}) of the roll solution $q_3(t)$ at different roll numbers v_3

v_3	0	1	2	3	4
Δ	0.1	0.3	0.3	0.3	0.3
ω_0	$\Omega/4$	$\Omega/4$	$\Omega/4$	$\Omega/4$	$\Omega/4$
a_{31}	−0.007	0.015	−0.052	0.090	0.024
a_{32}	0.001	−0.018	0.013	−0.010	0.188
a_{33}	1.472	1.243	0.823	0.878	−0.171
a_{34}	1.663	2.037	1.567	0.940	1.077
a_{35}	−0.008	0.006	−0.011	0.007	0.006
a_{36}	−0.006	0.342	0.199	−0.001	0.169
a_{37}	−0.111	−0.264	−0.093	−0.084	0.049
a_{38}	0.094	0.191	0.181	0.117	0.050
a_{39}	$<10^{-3}$	−0.010	0.012	0.039	0.063
a_{310}	−0.002	−0.011	−0.034	−0.062	−0.065
a_{311}	$<10^{-3}$	−0.037	−0.029	$<10^{-3}$	−0.003
a_{312}	$<10^{-3}$	−0.002	0.016	$<10^{-3}$	0.016
a_{313}	$<10^{-3}$	−0.001	0.018	0.012	0.012
a_{314}	$<10^{-3}$	−0.007	−0.019	−0.011	−0.018

Applying the periodicity condition (12b) to the solution (13b) yields

$$v_3 = \pm(s/r) \qquad (22)$$

where s is an arbitrary positive integer and where $r = 2\Omega/\omega_o$ denotes the ratio of the basic external to the basic internal frequency. Condition (22) indicates that the period of the superimposed oscillation and the period of the mean revolution have to be commensurable. The third condition for the existence of rotational modes consists in the proper adjustment of the cross-coupling Δ. The condition can be retrieved from the amplitude curves of the superimposed oscillation, represented in Fig. 4. As with the motion of class b each amplitude characteristic consists of two branches, which are diverging for larger amplitudes. The upper branch comprises the closed region of stable solutions as a subset, whereas the lower branch refers on its whole length to unstable solutions. All curves shown in Fig. 4 belong to rotational solutions of the resonance order $(p/r) = (2/4)$, since this was the only type of roll solution showing a stable behaviour inside the range $0 < \Delta < 1$. Rotational solutions of orders other than (2/4) have only been found in unstable form.

The expansion for $\Gamma(t)$, Eq. (7) did comprise the harmonic terms up to $n = 4$ for this study. According to condition (21) rotational modes with roll numbers $v_3 = \pm 1; \pm 2; \pm 3; \pm 4$ might exist and

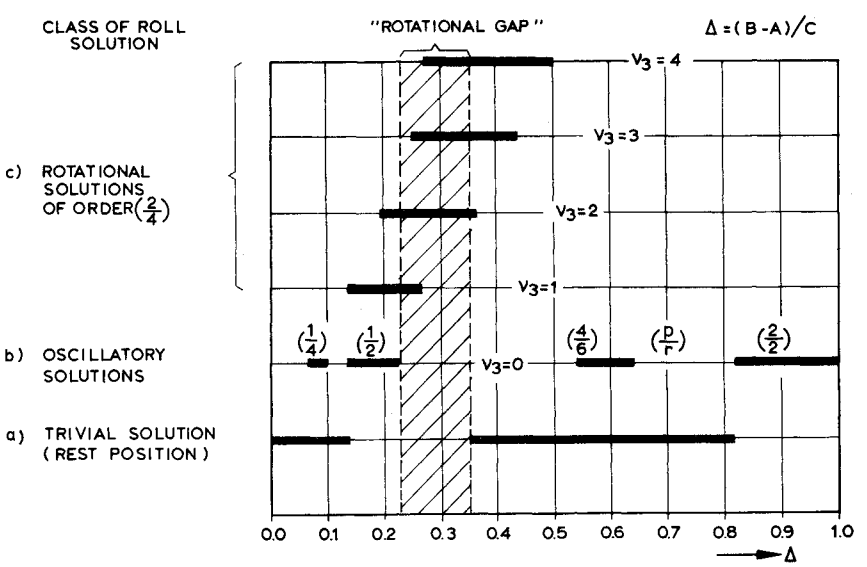

Fig. 5 Stability regions of the inertial cross-coupling Δ for the different classes of roll solutions, v_3—roll number in revolutions per orbit.

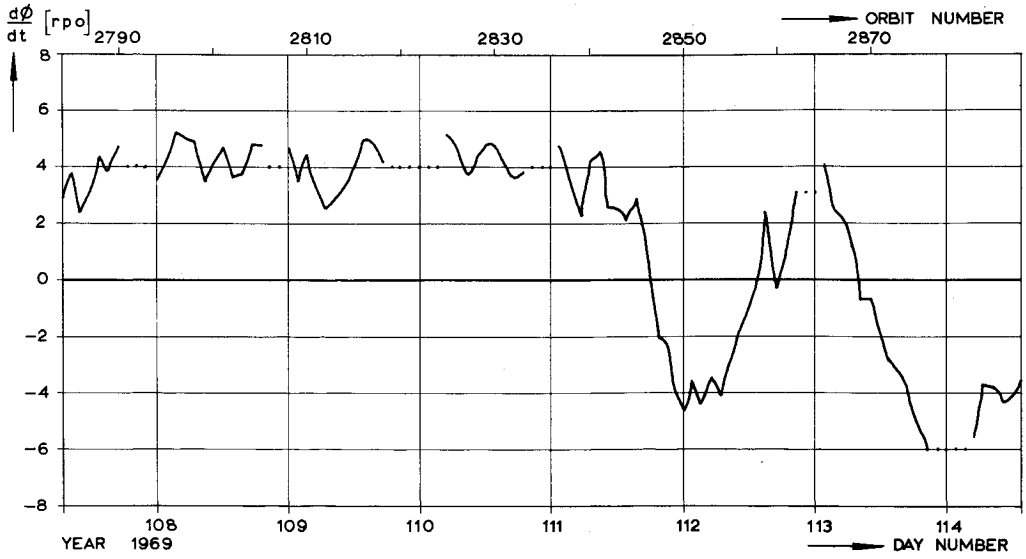

Fig. 6 Measured roll in revolution per orbit of the satellite ESRO IA for one week of increasing solar activity during April 1969.

have been verified numerically. Typical examples for the set of amplitudes $\{a_{3m}\}$ obtained for the 14-term solution of the roll angle are shown in Table 1. Here ω_o denotes the basic frequency $\omega_o = 2\Omega/r$ of the superimposed oscillation $q_3{}^*(t)$, a_{31} and a_{32} are the amplitudes of the basic sine-, respectively, cos-term of frequency $\omega_o = \Omega/4$, a_{33} and a_{34} are the amplitudes of the dominating terms with frequency $\omega_2 = \Omega/2$.

We finally shall discuss the influence of the slow parameter variations (frequency range 3) which are caused by the rotation of the Earth relative to the orbital plane. Computations for τ values in the range $(\Lambda_o - \Lambda_e - \pi/2) < \tau < (\Lambda_o - \Lambda_e + \pi/2)$ have shown the following results: 1) The effect of τ variations on the resonance amplitude $\hat{q}_3$ of the roll resonance oscillations is below 3%. 2) The coordinate q_1 (pitch angle shows mainly a phase shift for the fast time scale whereas the relative phase between q_1 and q_3 remains constant). 3) Only the coordinate q_2 (yaw angle) shows a remarkable amplitude change due to τ- variations. Two typical cases of oscillatory roll resonance $p/r = 1/2$, $\Delta = 0.25$, at $\tau_1 = (\Lambda_o - \Lambda_e)$ and $\tau_2 = (\Lambda_o - \Lambda_e + \pi/2)$ illustrate these findings.

$$\tau_1\colon\ \hat{q}_1 = 0.313,\quad \hat{q}_2 = 3.72\ 10^{-3},\quad \hat{q}_3 = 1.624 \quad \text{rad}$$
$$\tau_2\colon\ \hat{q}_1 = 0.306,\quad \hat{q}_2 = 3.10\ 10^{-2},\quad \hat{q}_3 = 1.602 \quad \text{rad}$$

The above results are explained by the particular structure of the potential energy term U which can be written as [see Eq. (5)]

$$U = U_1(q_1, q_2, t, \tau) + U_2(q_2, \tau) \tag{23}$$

Obviously U is independent of q_3 and no magnetic torque acts on the roll axis directly ($\partial U/\partial q_3 = 0$). The excitation of the resonance in frequency range 2 is caused only by $U_1(t)$. The part U_2 is a function of q_2 and the slow time τ only. Thus the dominant part of the energy exchange takes place between pitch motion and roll motion, which is also reflected in the different order of magnitude of q_1 and q_2 ($\hat{q}_1/\hat{q}_2 \geqslant 10$). $U_1(t)$ is a function of the in-plane component H_p. As seen from the expansions (6) it is rather the phase $\zeta(\tau)$ of $\Gamma(t)$ which is affected by τ- variations than the absolute value of H_p, which in turn explains result 2.

5. Selection of Optimal Parameters

As shown in the preceding section, the choice of the cross-coupling factor Δ is of decisive influence on the residual roll motion of the spacecraft. The question arises whether it is possible to select the factor Δ of the system in such a way that after decay of all transient motions one particular roll mode is being acquired. Such a policy would allow to control the roll motion in a passive way. In how far this ideal goal can be realized shall be discussed next.

To obtain a comprehensive view on the relations between the factor Δ and the state of the system, Fig. 5 has been drawn. It shows the stability region of Δ with respect to the total manifold of roll solutions. The figure demonstrates that the unique allocation of a certain stable roll solution to a particular Δ value is only possible in the exceptional case for $\Delta \to 1$, (absolute stability). For most parts of the Δ scale stability regions of different modes do overlap; that means the steady-state of the system depends on the systems parameter as well as on the initial conditions.

This result holds in particular for the rest position (class a-solution). As noted in section 4, the trivial solution $\Phi = 0 \pm n\pi$ is initially stable for the parameter Δ inside ST1 and ST2, but the region of stability with respect to $(\Phi, \dot{\Phi})$ is rather restricted. A relatively small amount of perturbing energy is sufficient to initiate an oscillatory or rotational roll motion. There is, however, the possibility to separate in a unique way the two *classes* of resonant roll motions by a suitable choice of the parameter Δ. Oscillatory roll solutions (class b) can be obtained under exclusion of any other stable mode for Δ values within $0.8 < \Delta < 1.0$. The roll solutions associated with the Δ region are of the order $\frac{2}{2}$, that means the dominating period is half the orbital period. As reaction to extreme perturbations the satellite might even pass through a transient phase of several full roll revolutions before the steady state oscillation will be re-established (absolute stability). The dominating amplitude of the oscillation can be retrieved from the curve $\frac{2}{2}$ of Fig. 3; the parameter region is identical with the region IN2 for the unstable trivial solutions.

Rotational roll solutions (class c) as a whole might be preselected under exclusion of stable class a and b motions. There is a small region of Δ-values $0.22 < \Delta < 0.35$, called the "rotational gap" where neither a stable rest position nor a stable oscillatory mode can exist. The only stable roll motions are rotational modes specified by its roll numbers $1 \leqslant |\nu_3| \leqslant 4$. That means by adjusting the crosscoupling factor Δ to a value within the rotational gap, the spacecraft will be kept in the state of a slow roll motion throughout its orbital life. This motion might be reversed due to environmental perturbations, but never comes to a halt. The lowest stable mode has an average rate of one revolution per orbit; the next higher stable modes are found at two, respectively three and four revolutions per orbit. The amplitudes of the superimposed oscillations can be taken from Fig. 4.

Summarizing the analytical results we find that in general not a particular roll solution but the class of resonant roll motions as a whole can be selected. By the proper choice of the moment of inertia ratio, the spacecraft can be forced to acquire either the state of stable oscillatory motions or the state of stable rotational motions. The class of rotational motions comprises a

small number of possible roll rates which constitute a discrete sequence.

In closing we shall report briefly on the practical experience made with this type of control. The policy outlined above has been applied to the ionospheric research satellites ESRO IA (AURORAE) and ESRO IB (BOREAS) launched in October 1968 and October 1969, respectively. Ground tests have shown that a roll rate of at least one revolution per orbit was required to keep the surface temperatures of the spacecraft within specified limits. Using additional trimming masses the moments of inertia of the lateral axes have been adjusted to achieve a crosscoupling factor inside the "rotational gap" near $\Delta = 0.3$. As seen from Fig. 4, the spacecraft should now perform rotational roll motions with roll numbers $2 \leqslant \nu_3 \leqslant 4$, i.e., between two and four revolutions per orbit. The actual flight performance is being demonstrated in Fig. 6, with an example of measured roll data from the satellite ESRO IA. The figure shows the average roll rate ($d\Phi/dt$) for an interval of about one week. For nearly five days, the roll rotation settled at a mean rate of four revolutions per orbit. During the following days of extremely high solar activity, the magnetic orientation as well as the roll behavior of the spacecraft has been seriously disturbed. For several times the satellite has been thrown out of its stable roll mode. Remarkably fast, however, and without coming to rest, the roll motion was reversed and acquired one of the stable inverse modes.

It has to be added that the satellite ESRO IA was launched close to the peak of the 11-yr cycle of solar activity. Data analysis still in progress has shown a strong correlation between solar activity (10.7-cm flux) and the following effects: 1) geomagnetic perturbations (ap index), 2) magnetic control error of the reference axis, 3) changes in roll modes. The same pattern has been observed for orbital perturbations of ESRO IA and other spacecrafts flown during 1968/69 under similar orbital conditions.[9] From these data, it has been concluded that the sudden increase in the density of the upper atmosphere (up to 500% during magnetic storms) rather than the actual geomagnetic perturbations are the source of the attitude perturbations.

In summarizing the experimental results, one finds that the optimized spacecraft is very well able to sustain a continuous roll motion for intervals of several days. At periods of high-level perturbations, e.g., during increased solar activity, the roll rate changes in a discontinuous manner but the satellite never stops rotating.

Appendix: The Potential Energy of The Satellite Dipole in The Earth Magnetic Field

Neglecting external sources, the potential of the Earth magnetic field can be represented as a scalar function V satisfying the Laplace equation div grad $V = 0$. The general solution for the boundary $r = R$ (mean earth radius) might be written in terms of spherical harmonics as

$$V = R \sum_{n=1}^{\infty} \sum_{m=0}^{n} \left(\frac{R}{r}\right)^{n+1} P_n^m\{\cos \nu\} (g_n^m \cos m\lambda + h_n^m \sin m\lambda) \quad \text{(A1)}$$

where ν and λ are colatitude and longitude of the geographical coordinate system; $P_n^m\{\cos \nu\}$ denotes the mth- order derivative of the Legendre polynominal P_n; g_n^m and h_n^m are the Gaussian coefficients which have been experimentally determined and tabulated.[10] The field intensity of the geomagnetic field is given as the gradient of V

$$\mathbf{H} = -\text{grad } V = [-\delta V/\delta r; -(1/r)\delta V/\delta \nu; -(1/r \sin \beta)\delta V/\delta \lambda]^T \quad \text{(A2)}$$

An approximation sufficiently accurate for attitude studies of satellites is obtained by truncating the expansion for V after the third term. What remains is the potential of a dipole M_e located at the center of the Earth and inclined at a fixed angle μ to the geographic polar axis. Relatively simple expressions for the local field gradient may be derived for satellites in circular and polar orbits.[11] Resolving the gradient (A2) in the geocentric orbit fixed system (x, y, z) defined in Fig. 7, and introducing the mean anomaly α and relative longitude Λ one finds from (A1) and (A2)

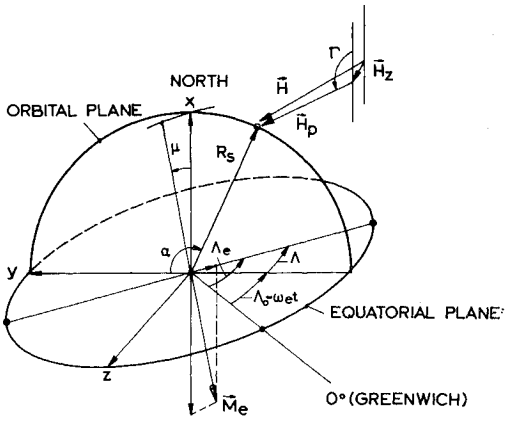

Fig. 7 Definition of the orbit fixed axis system (x, y, z) and position of the approximate dipole M_e of the geomagnetic field.

$$\begin{bmatrix} H_x \\ H_y \\ H_z \end{bmatrix} = -\frac{M_e}{2R_s^3} \begin{bmatrix} \cos\mu(1-3\cos 2\alpha)+3\sin\mu\cos\Lambda\sin 2\alpha \\ 3\cos\mu\sin 2\alpha+\sin\mu\cos\Lambda(1+3\cos 2\alpha) \\ -2\sin\mu\sin\Lambda \end{bmatrix} \quad \text{(A3)}$$

where the dipole quantities M_e, μ, Λ_e are given in terms of Gaussian coefficients as

$$M_e = R^3[(g_1^0)^2+(g_1^1)^2+(h_1^1)^2]^{1/2}$$
$$\tan\mu = [(g_1^1)^2+(h_1^1)^2]^{1/2}/g_1^0$$
$$\tan(\pi-\Lambda_e) = h_1^1/g_1^1$$

Coefficients computed from Vanguard III measurements,[12] yield the following dipole constants

$$M_e = 8.06\ 10^{25}\ \text{gcm}^3, \quad \mu = 11.45°, \quad \Lambda_e = 110.50°E$$

Furthermore we denote

$$\Lambda = \Lambda_e - \Lambda_o + \omega_e t \qquad \alpha = \alpha_o + \Omega t$$

with Λ_o, α_o orbital longitude of ascending node and mean anomaly α and relative longitude Λ one finds from (A1) and (A2) rate of the Earth, Ω mean orbital rate of the satellite, R_s radius of the satellite orbit.

The field intensity $\mathbf{H}^*$ expressed in the satellite fixed frame (X, Y, Z) is obtained by applying the orthogonal Euler-transformation defined by the angles (Ψ, Θ, Φ) to vector (A3),

$\mathbf{H}^* =$

$$\begin{bmatrix} (c\Phi c\Psi - c\Theta s\Psi s\Phi), & (c\Phi s\Psi + c\Theta c\Psi s\Phi), & s\Phi s\Theta \\ (-s\Phi c\Psi - c\Theta s\Psi c\Phi), & (-s\Phi s\Psi + c\Theta c\Psi c\Phi), & c\Phi s\Theta \\ s\Theta s\Psi, & -s\Theta c\Psi, & c\Theta \end{bmatrix} \begin{bmatrix} H_x \\ H_y \\ H_z \end{bmatrix} \quad \text{(A4)}$$

(s and c denote trigonometric sin and cos functions). The potential energy of the satellite's magnetic dipole $\mathbf{M}^*$ in the Earth magnetic field is obtained by integrating the magnetic torque $-\mathbf{T} = (\mathbf{M}^* \times \mathbf{H}^*)$ over the angular distance β between $\mathbf{M}^*$ and $\mathbf{H}^*$, (Fig. 2),

$$U = \int_0^{\beta} (\mathbf{M}^* \times \mathbf{H}^*)\, d\beta = -(\mathbf{M}^* \cdot \mathbf{H}^*) + C \quad \text{(A5)}$$

where $(\mathbf{M}^*.\mathbf{H}^*)$ denotes the scalar product of satellite dipole and Earth field intensity both measured in the body fixed frame. The magnetic moment of the satellite has been adjusted in direction of the $-Z$ axis, (Fig. 1), thus $\mathbf{M}^*$ is given as

$$\mathbf{M}^* = [0; 0; -M]^T \quad \text{(A6)}$$

From (A4), (A5), (A6) follows for U

$$U = MH_z^* = M\sin\Theta(H_x \sin\Psi - H_y \cos\Psi) + MH_z \cos\Theta + C$$

or

$$U = MH_p \sin\Theta \sin(\Psi - \Gamma) + MH_z \cos\Theta + C \quad \text{(A7)}$$

H_p represents the in-plane component of the local field intensity inclined at an angle Γ with respect to the x-axis, (Fig. 7):

$$H_p = |\mathbf{H}_p| = (H_x^2 + H_y^2)^{1/2}, \quad \Gamma = \arcsin(H_y/H_p)$$

where H_x, H_y, H_z are given by Eq. (A3). C denotes an integration constant which might be used to adjust the zero level of U.

The potential energy U, Eq. (A7) comprises periodic terms originating from the diurnal variations introduced by $\Lambda(\omega_e t)$ and orbital variations introduced by $\alpha(\Omega t)$. In order to separate the effect of the two frequencies on U, we shall expand H_p and Γ into Fourier series for Λ and α

$$H_p = H_{po}\left(1 + \sum_{n=0}^{\infty}\sum_{m=1}^{\infty}(h_n + k_{nm}\cos 2m\Lambda)\cos 2n(\alpha+\zeta)\right) \quad \text{(A8)}$$

$$\Gamma = \gamma_o - \sum_{n=1}^{\infty}\gamma_n \sin 2n(\alpha+\zeta) \quad \text{(A9)}$$

The field intensity component H_z normal to the orbital plane is obtained as

$$H_z = 0.1275\, H_{po} \sin\Lambda \quad \text{(A10)}$$

where the quantities H_{po}, γ_o and the phase ζ are given as

$$H_{po} = 1.249\ 10^{11}/R_s^3(Oe), \quad \gamma_o = -\zeta - 2\Omega t$$
$$\zeta = \arctan(0.203\cos\Lambda)$$

and the orbital radius R_s is being measured in kilometers. The coefficients h_n, k_{nm} and γ_n have been calculated on the basis of the aforementioned geomagnetic dipole constants; the most significant coefficients are compiled in Table 2.

Table 2 Coefficients of the Fourier expansion for H_p (Λ, α) and $\Gamma(\alpha)$

h_0	h_1	h_2	h_3
$-3.43\ 10^{-2}$	$-3.065\ 10^{-1}$	$-2.37\ 10^{-2}$	$-3.36\ 10^{-3}$
k_{01}	k_{11}	k_{21}	k_{31}
$-9.95\ 10^{-3}$	$-3.16\ 10^{-3}$	$-2.45\ 10^{-4}$	$-3.45\ 10^{-5}$
k_{02}	k_{12}	k_{22}	k_{32}
$-1.03\ 10^{-4}$	$-3.22\ 10^{-5}$	$\sim 10^{-5}$	$\sim 10^{-5}$
γ_1	γ_2	γ_3	γ_4
$3.34\ 10^{-1}$	$1.71\ 10^{-1}$	$9.23\ 10^{-2}$	$4.91\ 10^{-2}$

References

[1] Fischell, R. E., "Magnetic and Gravity Attitude Stabilisation of Earth Satellites," Rept. CM-996, May 1961, The John Hopkins Univ., Silver Spring, Md.

[2] Kammüller, R. W., "Nonlinear Resonant Roll Motion of Magnetically Oriented Satellites," *AIAA Journal*, Vol. 9, No. 4, April 1971, pp. 582–588.

[3] Kammüller, R. W., "Application of Variational Methods to Resonance Problems of Dynamic Systems," *Zeitschrift für Angewandte Mathematik und Physik*, Vol. 22, July 1971, pp. 714–724.

[4] The ESRO I Team, "ESRO I Spacecraft Description Document," ESRO TR-10, 1971, European Space Research and Technology Center, Noordwijk, Holland.

[5] Mitropolskii, Y. A., "Problems of the Asymptotic Theory of Nonstationary Vibrations," 1965, Israel Program for Scientific Translations, Jerusalem, Israel.

[6] Levinson, M., "Application of the Galerkin and Ritz Methods to Nonconservative Problems of Elastic Stability," *Zeitschrift für Angewandte Mathetik und Physik*, Vol. 17, 1966, p. 431.

[7] Kantorovitch, L. and Krylov, V., *Approximate Methods of Higher Analysis*, Wiley, New York, 1964.

[8] Marquardt, D., "An Algorithm for Least-Square Estimation of Nonlinear Parameters," *Journal of the Society for Industrial and Applied Mathematics*, Vol. 11, 1963, p. 431.

[9] Cook, G. E., "Variations in Exospheric Density 1967/68, as Revealed by Echo 2," *Planetary and Space Science*, Vol. 18, 1970, pp. 387–394.

[10] Leyhe, E. W., "Geomagnetic and Interplanetary Magnetic Field Environment of an Earth Satellite," TN D-1019, July 1962, NASA.

[11] Kammüller, R. W., "Passive Spin Control," ESRO TR-7, 1971, European Space Research and Technology Center, Noordwijk, Holland.

[12] Cain, J. C. et al., "Measurements of the Geomagnetic Field by the Vanguard III Satellite," TN D-1418, Oct. 1962, NASA.